NASA TECHNICAL NOTE

NASA TN D-7726

NASA TN D-7726

MISSION DESIGN FOR A BALLISTIC SLOW FLYBY OF COMET ENCKE 1980

by R. W. Farquhar, D. K. McCarthy, D. P. Muhonen, and D. K. Yeomans

Goddard Space Flight Center
Greenbelt, Md. 20771

NATIONAL AERONAUTICS AND SPACE ADMINISTRATION • WASHINGTON, D. C. • NOVEMBER 1974

1. Report No.	2. Government Accession No.	3. Recipient's Catalog No.
D-7726		

4. Title and Subtitle	5. Report Date
Mission Design for a Ballistic Slow Flyby of Comet Encke 1980	NOVEMBER-1974
	6. Performing Organization Code: 581
7. Author(s) R. W. Farquhar, D. K. McCarthy, D. P. Muhonen, and D. K. Yeomans	8. Performing Organization Report No.: G-7508
9. Performing Organization Name and Address: Goddard Space Flight Center, Greenbelt, Maryland 20771	10. Work Unit No.: 684-39-10-01
	11. Contract or Grant No.
	13. Type of Report and Period Covered: Technical Note
12. Sponsoring Agency Name and Address: National Aeronautics and Space Administration, Washington, D. C. 10546	14. Sponsoring Agency Code

15. Supplementary Notes

The information contained in this report was presented at the AIAA 12th Aerospace Sciences Meeting in Washington, D.C., on January 31, 1974.

16. Abstract

Preliminary mission analyses for a proposed 1980 slow flyby (7-9 km/s) of comet Encke are presented. Among the topics covered are science objectives, Encke's physical activity and ephemeris accuracy, trajectory and launch-window analysis, terminal guidance, and spacecraft concepts. The nominal mission plan calls for a near-perihelion intercept with two spacecraft launched on a single launch vehicle. Both spacecraft will arrive at the same time, one passing within 500 km from Encke's nucleus on its sunward side, the other cutting through the tail region. By applying a small propulsive correction about three weeks after the encounter, it is possible to retarget both spacecraft for a second Encke intercept in 1984.

The potential science return from the ballistic slow flyby is compared with other proposed mission modes for the 1980 Encke flyby mission, including the widely advocated slow flyby using solar-electric propulsion. It is shown that the ballistic slow flyby is superior in every respect.

17. Key Words (Selected by Author(s))	18. Distribution Statement
Comet intercept Solar probe	Unclassified–Unlimited CAT. 30

19. Security Classif. (of this report)	20. Security Classif. (of this page)	21. No. of Pages	22. Price*
Unclassified	Unclassified	32	$3.25

*For sale by the National Technical Information Service, Springfield, Virginia 22151.

CONTENTS

ILLUSTRATIONS

TABLES

MISSION DESIGN FOR A BALLISTIC SLOW FLYBY OF COMET ENCKE 1980

R. W. Farquhar, D. K. McCarthy, D. P. Muhonen
Goddard Space Flight Center

and

D. K. Yeomans
Computer Sciences Corporation

INTRODUCTION

It is now generally agreed that the next good cometary mission possibility is a flyby of Encke's comet in 1980.* However, there is little agreement on what is the most effective mission mode to accomplish the 1980 flyby. Three mission modes are currently being considered by NASA scientific and mission-planning groups. They are a slow flyby (~4 km/s) at about 0.80 AU from the sun using a solar-electric propulsion system; second, a ballistic slow flyby (7-9 km/s) near Encke's perihelion at approximately 0.34 AU; and third, a ballistic fast flyby (~20 km/s) at a heliocentric distance of 0.57 AU.

The ballistic slow-flyby concept was first presented in reference 2. In the original version, a single spacecraft flyby was envisioned. Now a new strategy has emerged that calls for sending a pair of spacecraft simultaneously past Encke. One spacecraft is targeted for a close pass of the comet's nucleus on its sunward side, while the other traverses the tail region. These spacecraft will be referred to as the coma probe and the tail probe, respectively. It is planned that one launch vehicle will launch both probes.

This paper describes the ballistic slow-flyby mission in detail and compares its advantages and disadvantages with the two other options listed above. In comparing the three mission modes, the primary evaluation criteria will be science value and realism of attaining mission objectives.

SCIENCE OBJECTIVES

A brief summary of the scientific objectives for the 1980 Encke flyby mission is given here. These objectives are divided into three categories: experiments relating to the nucleus and

*The first choice of the NASA-sponsored Comet and Asteroid Science Advisory Committee (1973) was the "Cometary Explorer" mission in 1976 to Grigg-Skjellerup and Giacobini-Zinner (reference 1). This mission is no longer a candidate due to budgetary and lead-time constraints.

coma region, tail experiments, and extended-mission goals. For comprehensive discussions of the cometary science objectives, see references 1, 3, 4, and 5.

The principal scientific objectives with regard to the comet's nuclear and coma regions are listed below.

- Determine the existence and nature of the cometary nucleus. If it does exist as a single coherent body, determine its size, shape, albedo, rotation rate, and surface features. Study the material ejection dynamics, and attempt to confirm the postulated existence of a halo of ice grains surrounding the nucleus.
- Describe the structure, composition, and motions of the cometary atmosphere. Establish the abundance, spatial distribution, kinematic behavior, and production rate of all those particles that are present in the coma with a particular emphasis on spatial resolution within the inner coma. The identity of the stable parent molecules must be known in order to understand how the unstable species (radicals) are formed.
- Determine the nature of the solar-wind, comet interaction. Two radically different types of interactions have been proposed. One model postulates a bow shock and contact surface analogous to those of the earth and its magnetosphere. The other suggests that the transition from supersonic to subsonic flow is continuous, is over a very broad region, and occurs without a bow shock.
- Study the basic mechanisms which produce ions and radicals. To fully understand the ionization processes, it will be necessary to measure the ion density, electron density, and energy distribution of charged particles within the coma. A survey of high frequency electric and magnetic field fluctuations is also essential to determine the importance of particle wave interactions.
- Determine the extent of the coma constituents as a function of heliocentric distance. Spectrophotometric measurements during the approach and departure phases will yield invaluable data on the time variation of the coma's structure including its hydrogen halo. The principal advantages of a comet probe for spectrophotometric experiments are higher intensities and spatial resolution.
- Survey the characteristics of dust grains. The size distribution, velocity distribution, and composition of dust particles are of particular interest.

Correlative measurements in the coma and tail regions are needed to fully understand cometary phenomena. In addition to the latter two items listed above, which should be extended to cover the tail region, there are two specific aims for tail experiments:

- Determine the physical origin of the ion tail. This includes the determination of where and how the tail materials become ionized and the flux of charged particles through the tail. The electron distribution should be determined. Direct measurements of mass per unit charge or energy per unit charge are also required.

- Study the properties of the plasma and magnetic field. Possibly establish whether or not the stylized variations of the tail structures (a) are associated with an imbedded magnetic field entrapped from the interplanetary medium, (b) are related to waves along the contact surface, or (c) are structures imbedded within the multiple neutral sheets that may exist in the cometary tail.

Typical payload complements for the coma and tail probes are listed in table 1. Although both spacecraft are spin stabilized, the coma probe is equipped with a despun platform which permits the accommodation of instruments that require specified orientations (for example, toward nuclear region or parallel to the relative velocity vector).

Table 1
Typical Payload Complement for Dual-probe Encke Flyby

Instrument	Coma Probe		Tail Probe
	Spinning Section	Despun Platform	
Imaging System		X	
Neutral Mass Spectrometer		X	
Ion Mass Spectrometer	X		X
UV Spectrometer		X	
Lyman-alpha Photometer		X	
DC Magnetometer	X		X
AC Magnetometer	X		X
Electron Analyzer	X		X
Plasma Analyzer	X		X
Electric Field Detector	X		X
Dust Detector	X		X
Dust Composition	X		X

Note that many of the instruments are well suited for interplanetary measurements during the extended-mission phase following the Encke encounter. The nominal spacecraft transfer orbit is quite similar to that of Helios A/B with the exception of the perihelion distance (0.34 AU instead of 0.30 AU) and the inclination (~10° instead of 0°). Because the Encke mission will occur near the maximum of solar activity, it will be possible to augment the Helios A/B investigations of the interplanetary medium that will be obtained during a period of minimum solar activity. Perihelion will occur when the two Mariner Jupiter-Saturn spacecraft are at 10 AU and presumably while other spacecraft are monitoring the solar wind at 1 AU; therefore, for the first time it will be possible to simultaneously study the solar wind over distances from 0.34 AU to 10 AU. Finally, simultaneous measurements

of the solar wind by two coordinated spacecraft close to the sun in 1980 represent a natural next step in the evolutionary sequence of solar-wind measurements. Such measurements are essential for the investigation of waves and instabilities, processes such as heat flux which depend on gradients, and generally for all processes for which space and time effects must be separated.

Another possible experiment for the twin-probe combination during the extended-mission phase is suggested by a recent article of Bertotti and Colombo (reference 6). This article states that it may be possible to obtain a more precise measurement of the sun's gravitational field from radio ranging measurements of two co-orbiting and closely-spaced space probes. The two probes are assumed to possess slightly different area-to-mass ratios, a property that could be used to eliminate the effect of unknown nongravitational forces in the tracking data. It is not clear that this technique would apply to the coma/tail probe combination, but further investigation is warranted.

COMET ENCKE

Of all the short-period comets, Encke has received the most attention in terms of its prior observation and orbit analyses. Since its discovery in 1786, it has been seen during 50 returns to perihelion; only one apparition (1944) has been missed since 1819. A plot of Encke's orbit along with its orbital elements for 1980 and 1984 are given in figure 1. Note that Encke's perihelion is almost coincident with its descending node. Another way of looking at Encke's orbit is depicted in figure 2. This representation, sometimes termed a bipolar plot, shows Encke's motion relative to a fixed sun-earth line for each apparition. From this plot it is easy to see why 1977 is a very poor year to observe Encke and, by the same token, why 1980 is a very good year.

The spectrum of comet Encke is strong in the lines of the molecules CN, C_2, and C_3, and it shows evidence of other molecular species commonly observed in cometary spectra. However, the continuum is especially faint, which indicates that Encke's dust content is rather low. (This does not mean that the meteoroid hazard for a spacecraft in the vicinity of Encke is negligible, because larger dust grains, which are capable of damaging the spacecraft, do not contribute significantly to the observed spectrum.) Typically a narrow ion tail starts to develop about 30 days before perihelion. At one time Encke's tail formation was thought to be related to solar activity, but now sightings and nonsightings of the tail are attributed to the geometrical variability of observing conditions.

Brightness Variation

Encke generally brightens perceptibly about six weeks before perihelion, and by the time it reaches perihelion it has enough brilliance to be classed as a naked-eye object. However, it is virtually impossible to view Encke near perihelion except for apparitions when the sun-comet elongation is close to its maximum value (for example, as will occur in 1980). Indeed, observations of Encke within ±10 days of perihelion are quite rare. Photometric

EPOCH	1980 DEC. 27.0
T	1980 DEC. 6.53014
q	0.3399399
e	0.8467556
Ω	334.19736
ω	185.97913
i	11.94598
EPOCH	1984 APR. 10.0
T	1984 MAR. 27.61142
q	0.3410024
e	0.8463282
Ω	334.18451
ω	185.99244
i	11.92741

⊕ Earth Positions at times of comet's perihelion.

P Comet perihelion point.

——— Above ecliptic.

– – – Below ecliptic.

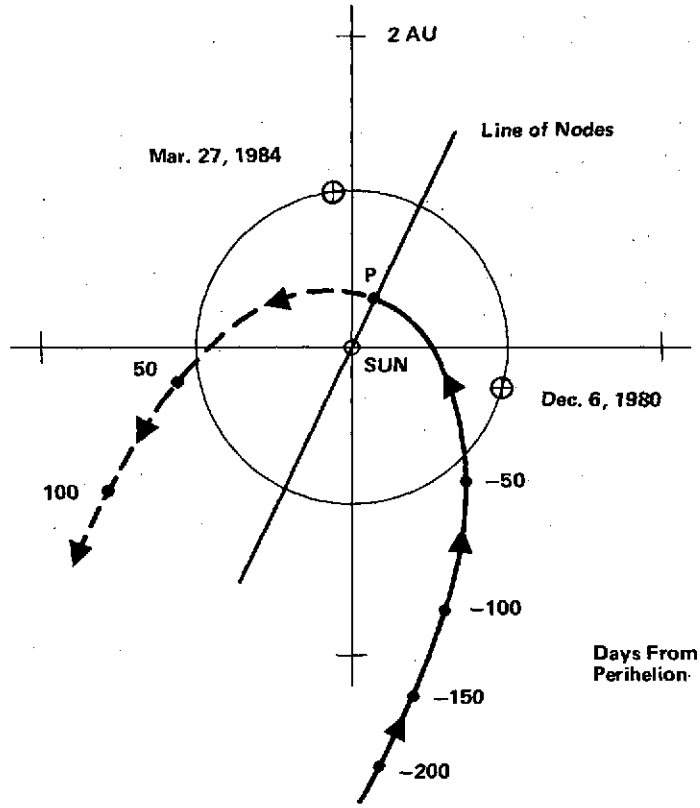

Figure 1. Orbit of comet Encke. (Orbital elements will be modified slightly when new observations become available.)

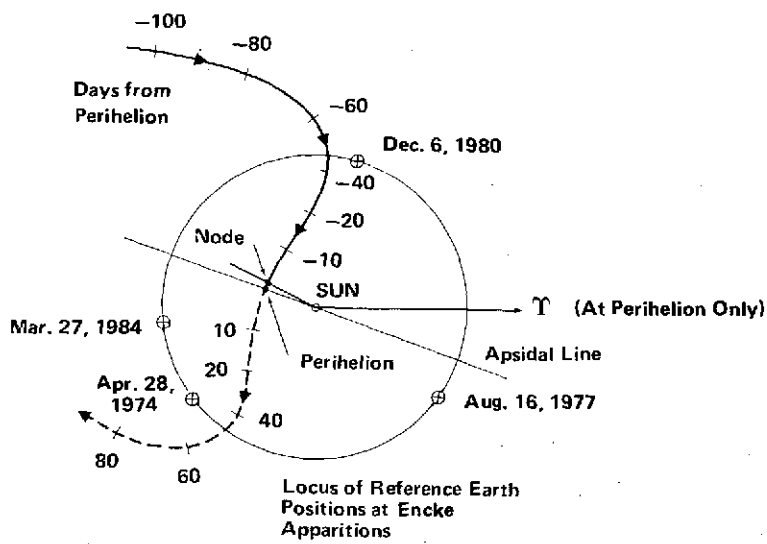

Figure 2. Orbit of comet Encke in bipolar coordinates.

data from this region does exist, but excessive sky brightness and atmospheric extinction have probably introduced large errors.

Post-perihelion observations have suggested that Encke's brightness variation is not completely symmetrical about perihelion, and that the post-perihelion absolute magnitude may be as much as one magnitude fainter than its pre-perihelion value.* It should be stressed that this is an average difference and does not indicate anomalous behavior of Encke in the vicinity of perihelion. In fact, as recently as 1964, Encke was actually brighter than predicted, some 23 days after perihelion (reference 9). When rapid fading has been observed, it has occurred about six to seven weeks after perihelion. A series of homogeneous observations (using same observer and same instrument) in May and June of 1974 could greatly increase knowledge of Encke's post-perihelion brightness variation.

Except for the possible pre- and post-perihelion asymmetry just mentioned, the photometric behavior of Encke is well represented by the magnitude equations (reference 10):

$$M_N = 16.0 + 5 \log \Delta + 5 \log r + 0.03 \beta \quad (1)$$

and

$$M_T = 11.5 + 5 \log \Delta + 15 \log r \quad (2)$$

where:

M_N = nuclear magnitude,

M_T = total magnitude,

Δ = distance between Encke and the observer in AU,

r = sun-Encke distance in AU,

β = phase angle (sun-comet-observer) in degrees.

Activity and Gas Density

A widely-held view concerning Encke's physical condition is that it is currently in the final stages of its evolutionary cycle, and that it will be entirely depleted of volatile substances in about 60 to 70 years (reference 11). The principal observational evidence supporting this view is based on:

- Photometric data that suggests a secular decrease in Encke's absolute magnitude of 3 to 4 magnitudes per century.
- A secular decrease in the transverse component of Encke's nongravitational acceleration since the early part of the 19th century.

It should be noted that the photometric data is rather crude, and conclusions concerning Encke's activity that have been derived from this data must be treated with some skepticism.

*This asymmetry has been estimated as 2 to 3 magnitudes by Kresak (reference 7); but, Sekanina (reference 8) has shown that Kresak's estimates are based on questionable analyses.

For example, the assumed decline in Encke's intrinsic brightness has been used to predict a death date of 1993 for Encke (reference 12). A later estimate has placed the death date at 2030 (reference 13). However, the validity of these predictions are rather doubtful in light of the predicted death dates given for other short-period comets; of the nine periodic comets mentioned in reference 12, five have already lived beyond their death dates. Furthermore, extrapolation of Encke's assumed secular brightness variation backwards in time leads to the conclusion that Encke must have been a very bright object prior to its discovery in 1786. Yet in spite of searches in the ancient Chinese dynastic records by Whipple and Hamid (reference 14), no earlier observations of Encke have been found.

Although the rate of the decline in Encke's absolute magnitude is still uncertain, the decrease of Encke's nongravitational acceleration is firmly established. In the most comprehensive analysis of Encke's nongravitational acceleration that has been completed to date, Marsden and Sekanina (reference 15) have found that the transverse component of the nongravitational acceleration reached a maximum value around the year 1820. It is also shown that the variation of this component was remarkably symmetrical about its maximum and appears to be following a sine curve. This new result supports the argument that the variation of Encke's nongravitational parameters is primarily due to a changing orientation of the nuclear rotation axis and less importantly to progressive depletion of volatile substances. Additional credence is given to this explanation by the recent discovery of Yeomans (reference 16) that the transverse nongravitational parameter of comet P/Kopff has passed smoothly through a change in sign.

New observational evidence that Encke is still an active comet was obtained in December 1970, when a large hydrogen cloud surrounding Encke was detected by a Lyman-alpha photometer on board the OGO-5 satellite (reference 17). The OGO-5 measurements of the gas production rate were used to scale the parent-molecule density profiles shown in figure 3. Because of the inverse-square law dependence on heliocentric distance, the parent production rate is highest near perihelion. However, as can be seen in the diagram, the density profile for 0.34 AU also drops off faster due to shorter photodissociation lifetimes at smaller heliocentric distances.

Delsemme (reference 18) has recently proposed a three-step mechanism for the brightness dependence on the heliocentric distance that has been observed for the hydrogen and hydroxyl clouds. Each step shows an inverse-square law dependence. The three steps are (1) vaporization of water snows from the cometary nucleus, (2) photodissociation of the water molecule into H and OH in their ground state, and (3) photoexcitation of H and OH and resonance fluorescence. Consequently, fluorescence of the daughter molecules will increase by a factor of 170 between 0.8 AU and 0.34 AU.

Recovery and Orbit Improvement

In reference 15 it is shown that five apparitions of comet Encke can be linked before the secular decrease in the nongravitational parameters begin to degrade the residuals. For the

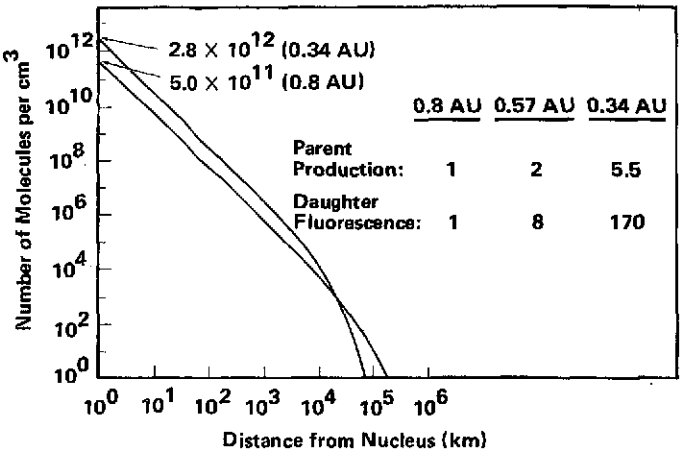

Figure 3. Parent-molecule (H_2O) density versus distance from the nucleus.

present analysis, the 5 returns to perihelion (1967 to 1980) are represented by 40 actual observations from August 2, 1967, through October 24, 1973, and by 28 additional postulated observations from October 24, 1973, through November 16, 1980. One observation was processed at each of the 1978 and 1979 opposition dates, and the 1980 recovery of the comet was assumed to occur on July 9. The postulated observation schedule was determined after considering the relative sun-earth-comet geometries, the available hours of dark observing time, as well as the apparent nuclear and total magnitudes for various dates.

The present error analysis of comet Encke assumes a 1-σ measurement noise of 3 arc seconds for both the right ascension and declination. This value is primarily due to the deviations of the comet's center-of-mass from the observed center-of-light. The 3-arc-second value is consistent with the mean residuals obtained for various orbit determinations for past apparitions of comet Encke. Due to comet Encke's relatively high nuclear activity, the appropriate noise value is somewhat higher than for most other short period comets.

The error analysis was initialized in 1967 by a state vector and appropriate values for the nongravitational parameters. The initial 8-by-8 covariance matrix was essentially infinite. Each set of observations was batch processed, and the updated covariance was propagated forward in time via the state transition matrix. All planetary perturbations were taken into account. The time history of the comet's error ellipsoid is presented in table 2. The first column represents the dates on which one ground-based observation was taken. The next six columns represent the 1-σ position errors (km) for the radial sun-comet direction ($\hat{r}$), the direction normal to the comet's orbital plane ($\hat{n}$), and the transverse direction defined by the cross product of the first two unit vectors ($\hat{T} = \hat{n} \times \hat{r}$). The columns headed by Δ, r, and θ represent the earth-comet distance in AU, the sun-comet distance in AU, and the sun-earth-comet angle in degrees, respectively. The a priori errors represent the forward propagation of the covariance matrix obtained by processing all observations from 1967 to 1974. Columns 5, 6, and 7 reflect the effect of each 1980 observation on the comet's error ellipsoid. The final ground-based observation on November 16 reduces the σ_r, σ_n

Table 2
Comet Encke Ephemeris Accuracy

Date 1980		A Priori One-sigma Errors in Radial, Normal, and Transverse Directions (km)*			Errors if 1980 Observations are Processed** (km)			AU		Deg. θ	Comments
		σ_r	σ_n	σ_T	σ_r	σ_n	σ_T	Δ	r		
July	9	4528	3900	5173	3352	1926	2471	2.4	2.3	72	Comet recovered.
	19	4705	3823	5105	2917	1737	2012	2.2	2.2	78	
	29	4897	3743	5047	2572	1567	1683	2.0	2.1	84	
Aug.	8	5104	3663	5000	2271	1406	1426	1.8	2.0	90	
	18	5330	3588	4965	1992	1249	1213	1.5	1.9	96	
	28	5577	3529	4947	1644	1146	1026	1.3	1.8	101	
Sept.	7	5849	3503	4946	1469	945	836	1.1	1.7	107	
	17	6151	3543	4959	1217	799	710	0.9	1.6	111	
	27	6490	3715	4968	968	658	564	0.7	1.4	114	
Oct.	7	6869	4124	4929	724	524	427	0.5	1.3	112	
	17	7294	4861	4798	504	400	313	0.4	1.1	103	
	27	7757	5826	4766	387	308	264	0.3	1.0	77	
Nov.	6	8204	6635	5682	391	269	273	0.3	0.8	45	
	16	8371	6446	8800	416	249	359	0.5	0.6	29	Last comet observation.
	26	6954	4826	14022	401	234	579	0.7	0.4	23	
Dec.	7	1299	3501	17872	150	246	888	1.0	0.3	19	Intercept.
Dec.	7				152	251	888				Errors at intercept if 1978 and 1979 measurements are excluded.
Dec.	7				139	186	674				Errors at intercept if measurements are taken at 5 day intervals in 1980.

* Last observation processed was toward end of 1974.
** Evolution of one-sigma errors if one ground based observation is processed at 10 day intervals from July 9 to November 16. Measurement noise = 3 arc seconds.

and σ_T components to 416, 249, and 359 km. In the absence of further observations, σ_T grows to 888 km and σ_r shrinks to 150 km at the December 7, 1980, intercept. This behavior is due primarily to the dynamic evolution of the error ellipsoid in the absence of observations. On December 7, 1980, the σ_T component is along track and because the comet's velocity is approximately 6×10^6 km/day at perihelion, the σ_T corresponds to an error in perihelion passage time of 1.5×10^{-4} day. This result is compatible with results obtained from differential corrections using recent observations. Excluding the 1978 and 1979 opposition observations has a negligible effect upon the final intercept errors. However, by taking 1980 observations at 5-day intervals between July 9 and November 16, the final intercept errors are reduced to 139, 186, 674 km (σ_r, σ_n, σ_T). These results underscore the fact that while observations made during past apparitions define the mean motion and the nongravitational parameters, it is the 1980 observations that contribute most strongly to the reduction of comet Encke's ephemeris uncertainty.

MISSION DESCRIPTION

Because the parent molecule and ion densities are highest when Encke is near its perihelion, an intercept in this region would offer the best chance of obtaining an accurate measurement of these particles above the instrumental threshold. Detection of the characteristic molecular bands of the daughter molecules is also easier near perihelion because the intensities increase with decreasing heliocentric distance, displaying an inverse 6th-power variation. However, perhaps the most significant factor in determining the optimum location for the intercept is the relative velocity between the comet and the spacecraft at encounter. It is important to achieve a low flyby speed in order to:

- Increase chances for early detection of Encke's nucleus.
- Maximize time available for in situ measurements of the cometary atmosphere.
- Reduce smear in imaging requirements.
- Minimize probability of neutral-molecule impact fragmentation.

Two factors just mentioned, high cometary activity and low flyby speed, are quite often mutually exclusive. However, the 1980 Encke opportunity is unique in the sense that it permits a minimum-speed flyby in the perihelion region. As shown in figure 4, the flyby speed is minimized near perihelion and increases rather sharply in the pre-perihelion region. The increase is not as drastic in the post-perihelion region, but other factors such as higher launch energy requirements and longer communication distances argue against intercepts more than a few days past perihelion. Actually several variables are involved in the determination of a nominal mission profile. It is the purpose of this section to investigate near-perihelion ballistic intercepts in sufficient detail to form the parametric data-base that is needed for the selection of a preferred mission mode.

Mission Profile and Launch Window

A typical mission profile for a near-perihelion intercept of Encke is summarized in figure 5. Note that the launch occurs when the earth is almost coincident with Encke's nodal line. It is this fortuitous circumstance that enables the spacecraft to follow a transfer trajectory in essentially the same plane as Encke's orbit, thus reducing the out-of-plane component of the relative velocity vector. Another noteworthy feature of the transfer trajectory is that it closely approximates a Hohmann Transfer, which means that the launch-energy requirement is near its minimum value for a same-plane perihelion intercept.

Variations of several key mission parameters are listed in table 3 as functions of the launch date and intercept date. The exact time of the intercept on each day has been chosen as 10:00 GMT, to maximize coverage from the 100-meter antenna at Effelsberg, Germany. Although several combinations of launch and intercept dates provide flyby speeds under 9 km/second, other mission constraints must also be considered before a nominal launch window can be selected. A possible two-week launch window for a launch energy, C_3, below 92 km^2/s^2 begins on August 16 and ends on August 30, 1980. The intercept dates from December 3 to 8 provide flyby speeds between 7.60 and 9.03 km/second.

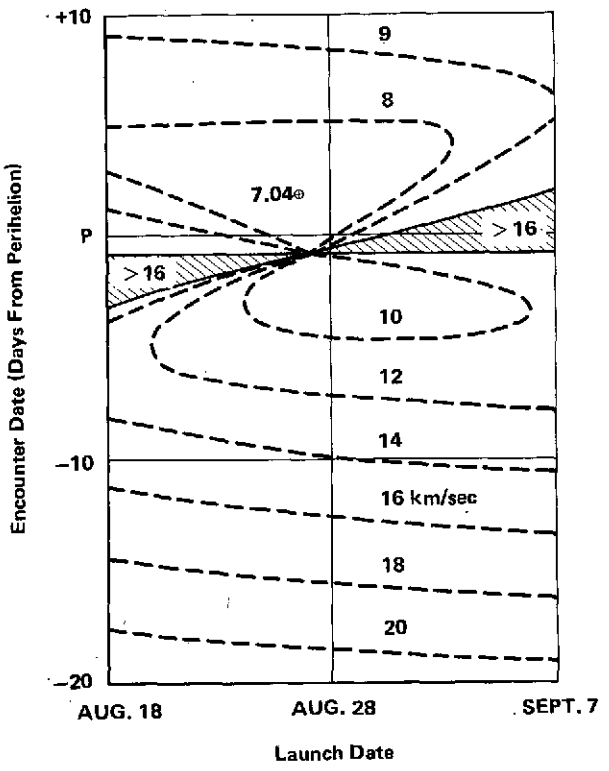

Figure 4. Relative-velocity contours for 1980 Encke encounter.

As mentioned earlier, the mission plan calls for two spacecraft to be launched on a single launch vehicle. A Titan/Centaur appears to be well suited for this task. The payload capability of this vehicle is indicated in figure 6. It is estimated that the payload system weight for the two-spacecraft combination will not exceed 760 kg, which corresponds to a launch-energy capability of $C_3 = 92\ km^2/s^2$ for the Titan/Centaur vehicle. This capability can be increased to about $C_3 = 108\ km^2/s^2$ by adding a solid stage (TE 364-3) to the Titan/Centaur. However, because of the larger injection errors incurred with a solid stage, a launch without a solid stage is preferable.

After separation from the Centaur upper stage, both spacecraft are spin stabilized and their spin axes are aligned so that they are perpendicular to the transfer-orbit plane. When the spin-axis orientation maneuvers are completed, inflight calibration measurements of the coma probe's imaging system can be initiated. An added bonus of the twin-probe scheme is that the tail probe could be used for these calibration measurements. In fact, simulations of the difficult nucleus-acquisition phase of the mission could also be attempted.

The first midcourse correction is scheduled for 10 days after launch. This correction is used to eliminate the launch vehicle injection dispersions. A second midcourse correction at 50 days after launch accounts for the improved comet ephemeris estimates and execution errors from the first correction. At that time the tail probe will be targeted for an

Launch Date	Aug. 26, 1980
Intercept Date	Dec. 6, 1980
Flight Time	102 Days
Launch Energy	88.0 km^2/sec^2
At Intercept	
Relative Velocity	8.14 km/sec
Sun Distance	0.34 AU
Earth Distance	1.02 AU
Transfer Orbit	
Perihelion	0.34 AU
Aphelion	1.01 AU
Inclination	9.33°
Period	202.5 Days

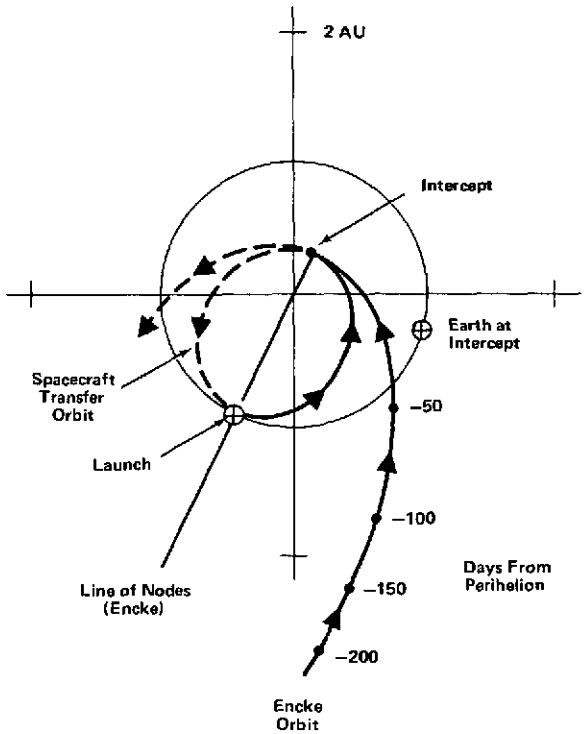

Figure 5. Typical mission profile.

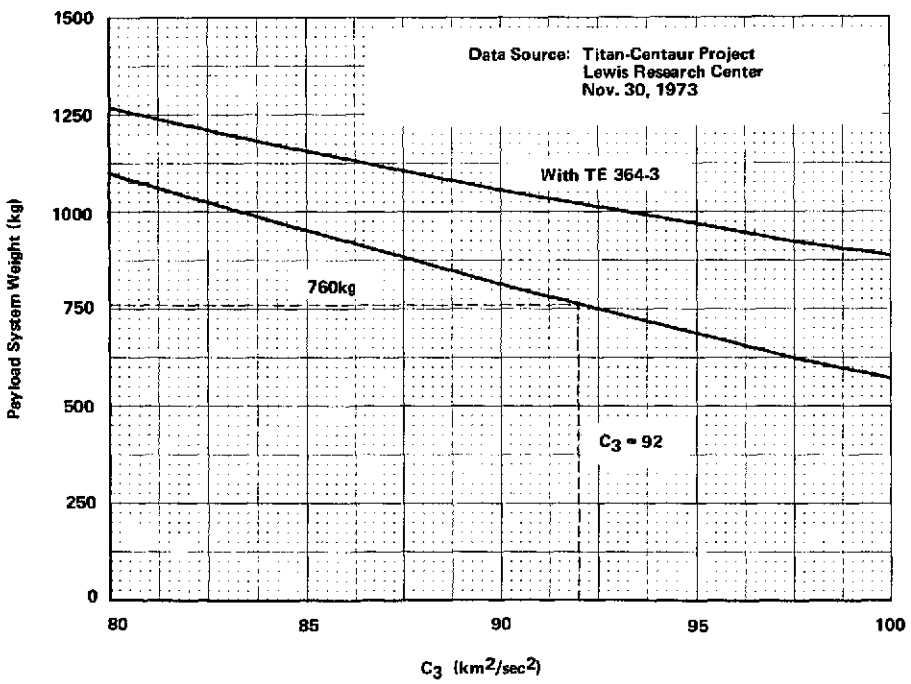

Figure 6. Titan-3E/Centaur D-1T performance.

Table 3
Launch-window Data for Near-perihelion Intercept*

Launch Date 1980	Launch Parameters		Transfer Orbit		Comet-Encounter Parameters		
	C_3	DLA	INC.	Period	V_{REL}	ELEV.	Phase
Intercept Date: Dec. 3, 1980 Sun-Comet Elongation: 20.8°					Earth Distance: 0.920 AU Sun Distance: 0.350 AU		
Aug. 27	97.7	5.8	12.4	204.3	9.16	-3.4	43.1
28	94.4	4.5	11.6	204.3	9.09	2.5	43.5
29	91.7	3.4	10.9	204.3	9.09	7.8	44.4
30	89.6	2.4	10.3	204.4	9.14	12.4	45.6
31	88.0	1.4	9.8	204.4	9.23	16.6	47.0
Sept. 1	86.8	0.6	9.3	204.6	9.34	20.2	48.3
2	86.0	-0.2	8.9	204.7	9.47	23.5	49.7
3	85.6	-1.0	8.5	204.9	9.61	26.4	51.1
4	85.4	-1.7	8.1	205.1	9.75	29.0	52.3
5	85.6	-2.3	7.8	205.4	9.89	31.3	53.5
6	86.0	-2.9	7.5	205.7	10.03	33.4	54.6
7	86.6	-3.4	7.2	206.1	10.17	35.3	55.7
8	87.6	-3.9	7.0	206.6	10.30	37.0	56.6
9	88.8	-4.4	6.7	207.1	10.43	38.6	57.5
10	90.2	-4.9	6.5	207.6	10.56	40.1	58.3
11	91.9	-5.3	6.3	208.2	10.69	41.4	59.1
12	93.9	-5.6	6.1	208.9	10.80	42.7	59.8
Intercept Date: Dec. 4, 1980 Sun-Comet Elongation: 20.4°					Earth Distance: 0.951 AU Sun Distance: 0.345 AU		
Aug. 27	100.8	6.0	12.8	203.5	8.56	-6.7	50.8
28	94.4	3.8	11.4	203.5	8.47	4.9	51.2
29	90.0	1.8	10.2	203.5	8.62	14.1	52.8
30	86.8	0.1	9.3	203.6	8.87	21.3	54.8
31	84.6	-1.3	8.5	203.7	9.17	27.0	56.8
Sept. 1	83.1	-2.6	7.9	203.8	9.47	31.5	58.7
2	82.2	-3.7	7.3	204.0	9.76	35.3	60.3
3	81.7	-4.6	6.8	204.2	10.04	38.3	61.8
4	81.6	-5.5	6.4	204.4	10.30	40.9	63.1
5	81.8	-6.2	6.0	204.7	10.54	43.1	64.2
6	82.3	-6.8	5.7	205.0	10.76	45.0	65.2
7	83.1	-7.4	5.4	205.4	10.97	46.7	66.1
8	84.2	-7.9	5.1	205.9	11.16	48.1	66.9
9	85.5	-8.4	4.9	206.3	11.33	49.4	67.6
10	87.1	-8.8	4.7	206.9	11.49	50.6	68.3
11	88.9	-9.1	4.5	207.5	11.64	51.7	68.8
12	91.1	-9.5	4.3	208.2	11.78	52.6	69.3

* ***Definitions:***

C_3	Launch energy in km^2/sec^2
DLA	Declination of launch asymptote in degrees
INC.	Inclination of transfer orbit in degrees
Period	Period of transfer orbit in days
V_{REL}	*Relative velocity* in km/sec
ELEV.	Elevation angle in degrees (angle between S/C orbit plane and relative-velocity vector)
Phase	Phase angle in degrees (measured from sun-comet line to relative-velocity vector)

Table 3
Launch-window Data for Near-perihelion Intercept* (Continued)

Launch Date 1980	Launch Parameters		Transfer Orbit		Comet-Encounter Parameters		
	C_3	DLA	INC.	Period	V_{REL}	ELEV.	Phase
Intercept Date: Dec. 5, 1980 Sun-Comet Elongation: 20.0°					Earth Distance: 0.983 AU Sun Distance: 0.341 AU		
Aug. 27	—	—	—	—	—	—	—
28	87.0	-0.4	9.2	202.9	8.50	23.0	62.0
29	78.4	-6.6	6.1	202.9	10.28	42.9	67.8
30	75.4	-9.9	4.6	203.0	11.46	50.4	70.7
31	74.3	-12.0	3.7	203.1	12.22	54.4	72.4
Sept. 1	74.0	-13.3	3.1	203.2	12.74	56.8	73.6
2	74.2	-14.2	2.7	203.4	13.12	58.5	74.5
3	74.7	-14.8	2.3	203.6	13.40	59.8	75.2
4	75.4	-15.3	2.1	203.9	13.62	60.8	75.8
5	76.3	-15.7	1.9	204.2	13.80	61.6	76.4
6	77.4	-15.9	1.7	204.5	13.94	62.3	76.8
7	78.7	-16.1	1.6	204.9	14.05	62.7	77.2
8	80.2	-16.2	1.4	205.3	14.15	63.3	77.6
9	81.9	-16.3	1.3	205.8	14.23	63.8	77.9
10	83.9	-16.4	1.3	206.4	14.30	64.2	78.2
11	86.0	-16.4	1.2	207.0	14.36	64.6	78.4
12	88.4	-16.4	1.1	207.7	14.42	64.9	78.7
Intercept Date: Dec. 6, 1980 Sun-Comet Elongation: 19.5°					Earth Distance: 1.015 AU Sun Distance: 0.340 AU		
Aug. 15	80.8	-13.7	3.7	204.1	12.69	53.0	69.9
16	80.2	-13.2	3.9	203.8	12.44	52.5	70.2
17	79.7	-12.5	4.1	203.6	12.18	51.8	70.5
18	79.3	-11.8	4.4	203.4	11.89	51.0	70.8
19	79.0	-11.0	4.7	203.2	11.58	49.9	71.0
20	79.0	-10.1	5.0	203.1	11.23	48.6	71.1
21	79.2	-9.1	5.5	202.9	10.84	46.8	71.2
22	79.7	-7.9	6.0	202.8	10.41	44.6	71.1
23	80.6	-6.5	6.5	202.7	9.92	43.2	71.0
24	82.1	-4.9	7.3	202.6	9.37	37.5	70.6
25	84.4	-2.9	8.2	202.5	8.77	31.7	70.0
26	88.0	-0.6	9.3	202.5	8.14	23.1	69.3
27	93.7	2.3	10.9	202.5	7.62	10.1	68.6
28	103.2	5.9	13.0	202.5	7.56	-9.5	69.3
29	120.3	10.4	16.1	202.5	8.83	-34.6	73.0
30	154.7	15.6	21.0	202.6	12.79	-59.0	78.7

*** Definitions:**

C_3 — Launch energy in km^2/sec^2

DLA — Declination of launch asymptote in degrees

INC. — Inclination of transfer orbit in degrees

Period — Period of transfer orbit in days

V_{REL} — Relative velocity in km/sec

ELEV. — Elevation angle in degrees (angle between S/C orbit plane and relative-velocity vector)

Phase — Phase angle in degrees (measured from sun-comet line to relative-velocity vector)

Table 3

Launch-window Data for Near-perihelion Intercept* (Concluded)

Launch Date 1980	Launch Parameters		Transfer Orbit		Comet-Encounter Parameters		
	C_3	DLA	INC.	Period	V_{REL}	ELEV.	Phase
Intercept Date: Dec. 7, 1980 Sun-Comet Elongation: 19.0°					Earth Distance: 1.047 AU Sun Distance: 0.341 AU		
Aug. 15	86.5	-8.6	6.1	203.6	10.45	44.9	73.2
16	86.1	-7.9	6.3	203.4	10.20	44.8	73.7
17	85.7	-7.3	6.6	203.2	9.94	42.5	74.2
18	85.5	-6.6	6.9	203.0	9.68	41.0	74.6
19	85.5	-5.8	7.2	202.8	9.40	39.3	75.1
20	85.7	-4.9	7.5	202.6	9.12	37.2	75.5
Aug. 21	86.2	-4.0	7.9	202.5	8.82	34.7	75.9
22	86.9	-3.1	8.3	202.4	8.52	31.8	76.3
23	87.9	-2.0	8.8	202.3	8.22	28.3	76.6
24	89.3	-0.9	9.4	202.2	7.92	24.0	77.0
25	91.2	0.4	10.0	202.2	7.64	18.8	77.4
26	93.6	1.8	10.7	202.1	7.39	12.5	77.9
27	96.8	3.2	11.5	202.1	7.23	4.9	78.5
28	100.9	4.9	12.4	202.2	7.20	-4.2	79.2
29	106.3	6.6	13.5	202.2	7.37	-14.7	80.2
30	113.4	8.6	14.8	202.3	7.85	-26.2	81.5
Intercept Date: Dec. 8, 1980 Sun-Comet Elongation: 18.5°					Earth Distance: 1.079 AU Sun Distance: 0.344 AU		
Aug. 15	91.0	-5.8	7.5	203.2	9.23	39.1	79.5
16	90.5	-5.3	7.7	203.0	9.03	37.7	80.2
17	90.1	-4.6	7.9	202.8	8.82	36.2	81.0
18	89.9	-4.0	8.2	202.7	8.61	34.4	81.7
19	89.9	-3.3	8.5	202.5	8.40	32.4	82.5
20	90.0	-2.6	8.8	202.4	8.20	30.2	83.2
21	90.4	-1.9	9.1	202.2	7.99	27.6	84.0
22	90.9	-1.1	9.4	202.1	7.79	24.7	84.8
23	91.7	-0.3	9.8	202.0	7.60	21.4	85.6
24	92.7	0.6	10.2	202.0	7.42	17.7	86.4
25	94.1	1.5	10.6	201.9	7.27	13.4	87.2
26	95.8	2.5	11.1	201.9	7.15	8.6	88.0
27	97.9	3.5	11.6	201.9	7.07	3.2	88.8
28	100.5	4.6	12.2	202.0	7.05	-2.8	89.6
29	103.6	5.7	12.9	202.0	7.12	-9.4	90.4
30	107.4	6.9	13.6	202.1	7.29	-16.5	91.0

* **Definitions:**

C_3	Launch energy in km^2/sec^2	V_{REL}	Relative velocity in km/sec
DLA	Declination of launch asymptote in degrees	ELEV.	Elevation angle in degrees (angle between S/C orbit plane and relative-velocity vector)
INC.	Inclination of transfer orbit in degrees	Phase	Phase angle in degrees (measured from sun-comet line to relative-velocity vector)
Period	Period of transfer orbit in days		

interception with the tail region approximately 10,000 km from the nucleus.* Simultaneous with the passage of the tail probe through the tail, the coma probe will pass through the comet head immediately in front of the nucleus. The final corrections will take place two days before the encounters. The ΔV requirements for the planned midcourse corrections are listed in table 4.

*The 10,000-km distance is used for planning purposes. The actual miss distance for the tail probe will be decided by the Science Working Team.

Table 4
Typical Midcourse Corrections

Maneuver Execution Errors (3-σ)	
Magnitude	4.5%
Pointing	1.5°

ΔV Requirements (3-σ)	Meters per Second
MCC #1 (Launch + 10 Days)	12.9
MCC #2 (Launch + 50 Days)	6.0*
MCC #3 (Launch + 85 Days)	2.9
MCC #4 (Encounter - 2 Days)	13.6
Total Midcourse Corrections	25.1**

*Tail probe will require additional 2.7 meters per second.
**Statistical sum.

Approach and Encounter Phase

Spacecraft trajectories before and after encounter are shown in figures 7-9. The period covered in each case is from E -14 days to E + 10 days. Nuclear magnitudes of Encke as seen from the spacecraft were obtained by applying equation 1. Additional encounter parameters are given in table 3.

Note the favorable geometry for spectrophotometric measurements of the coma/tail region before and after encounter. This geometry coupled with Encke's increased brightness near perihelion should provide valuable data concerning evolutionary behavior of Encke's coma and tail constituents.

The unique advantages of the near-perihelion encounter geometry and the dual-probe strategy are graphically illustrated in figure 10. For the coma probe, which will pass the nucleus on its sunward side, the principal advantages are listed below.

- Excellent imaging geometry. It will be possible to obtain a maximum number of high-resolution pictures when the spacecraft is closest to Encke's nuclear region. Pictures can be taken during approach *and* departure at acceptable phase angles, and with minimum solar interference. As a matter of fact, the most favorable phase angles occur when the distances between the spacecraft and the nucleus are smallest. Furthermore, the illumination of the nucleus is greatest near perihelion.

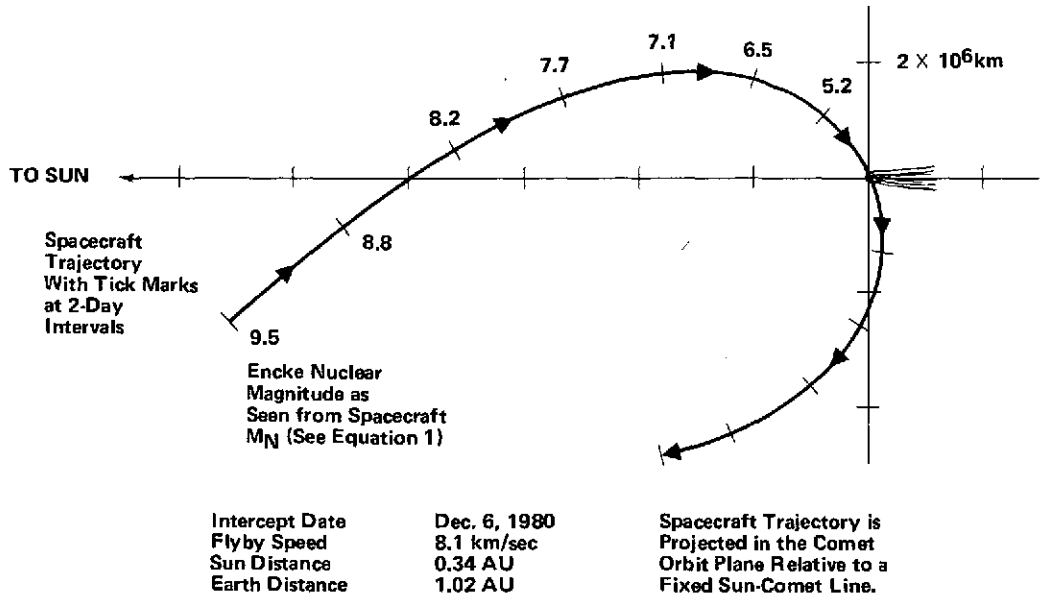

Intercept Date	Dec. 6, 1980	Spacecraft Trajectory is
Flyby Speed	8.1 km/sec	Projected in the Comet
Sun Distance	0.34 AU	Orbit Plane Relative to a
Earth Distance	1.02 AU	Fixed Sun-Comet Line.

Figure 7. Encounter geometry for perihelion intercept.

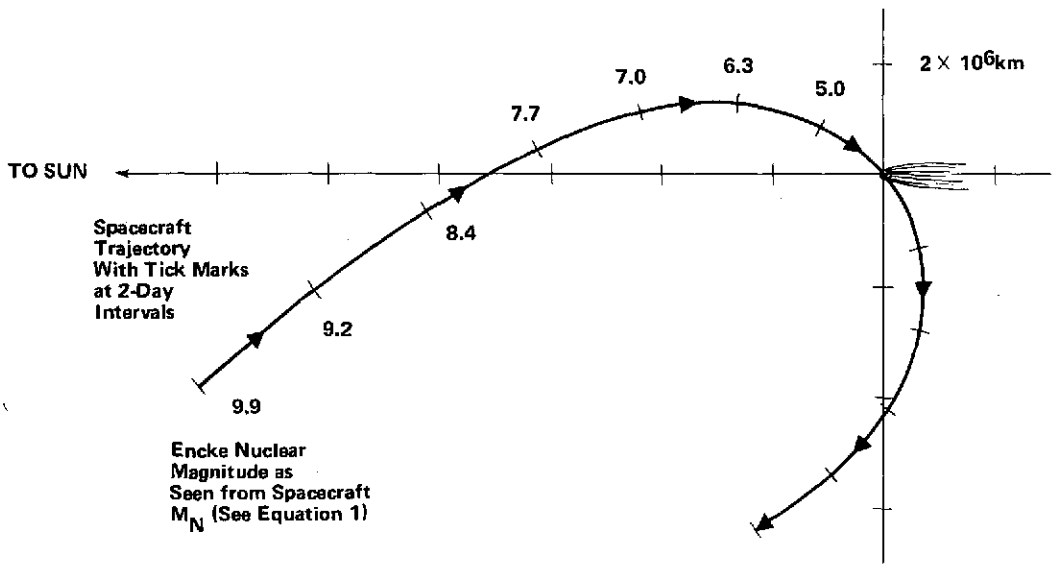

Intercept Date	Dec. 4, 1980	Spacecraft Trajectory is
Flyby Speed	8.6 km/sec	Projected in the Comet
Sun Distance	0.35 AU	Orbit Plane Relative to a
Earth Distance	0.95 AU	Fixed Sun-Comet Line.

Figure 8. Encounter geometry for intercept at P - 2 days.

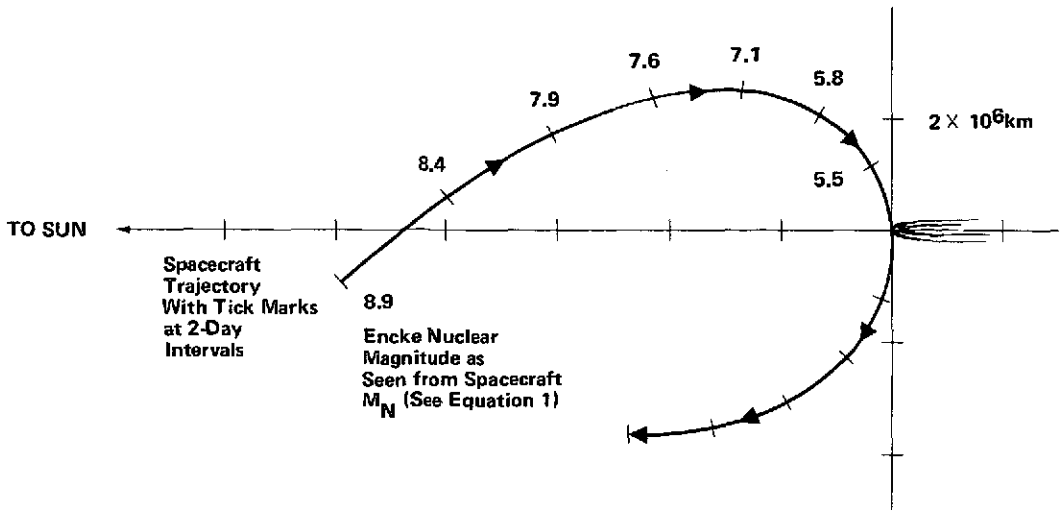

Figure 9. Encounter geometry for intercept at P + 2 days.

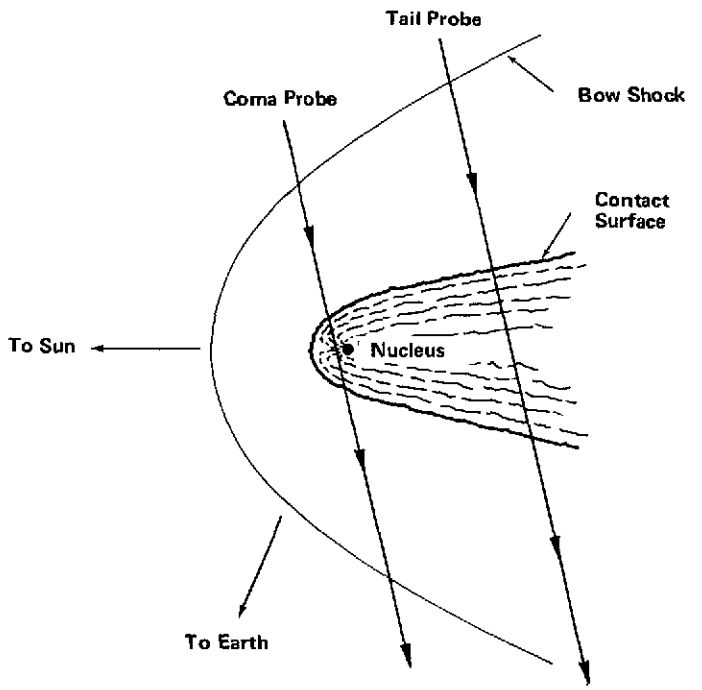

Figure 10. Dual-probe encounter geometry (not to scale).

- Double crossings of the bow shock and contact surface. This will lead to a more conclusive determination of the existence and location of these features.
- Cross-sectional mapping of the interaction region immediately in front of the nucleus. Details of the jet structure in this region are needed to fully understand the nature of the solar-wind comet interaction.

The coma-probe measurements will be significantly enhanced by the simultaneous data from the tail probe. This will extend the mapping of Encke's structure to its longitudinal axis and prevent possible confusion between spatial and temporal variations.

Terminal Guidance

Early detection of Encke's nucleus from the approaching spacecraft is necessary to ensure that enough time is available for terminal guidance operations. Although current spacecraft imaging systems have detected stars as dim as magnitude 9.3 (with nonreal-time processing), Mariner-9 flight experience (references 19 and 20) suggests that the detection threshold for Encke's nucleus will not be much better than magnitude 8.0. Even this threshold value could prove to be somewhat optimistic because stray light from Encke's coma might complicate nuclear detection. However, assuming that magnitude 8.0 is realistic, figures 7, 8, and 9 show that Encke's nuclear region is observable from the spacecraft 9 to 10 days before encounter.

The nominal terminal-guidance strategy calls for a series of optical measurements of Encke's angular position from the spacecraft beginning as soon as Encke's nucleus can be detected and ending at E -3 days. These measurements will be used to further reduce the uncertainties in Encke's ephemeris. A final spacecraft maneuver, which incorporates all comet and spacecraft tracking measurements up to E -3 days, will be executed at E -2 days.

Results of a preliminary analysis of typical spacecraft targeting errors with and without onboard measurements are presented in figure 11. The substantial improvement in targeting accuracy when onboard measurements are employed is apparent. However, it will be shown below that the targeting error without onboard measurements is still sufficiently small to guarantee satisfactory science return.

Extended Mission

When experiments connected with the Encke encounter have been completed, the science payload of the dual-probe combination will concentrate on measurements of the interplanetary medium from 0.34 AU to 1.0 AU. As mentioned above (see section on science objectives), unique investigations of the solar wind will be made possible by simultaneous measurements from these two co-orbiting spacecraft. A plot of the spacecraft's trajectory during the first 400 days of the extended mission phase is shown in figure 12. Note that periods of communications blackout due to solar interference are usually avoided because the spacecraft's orbit-plane is slightly inclined to the ecliptic.

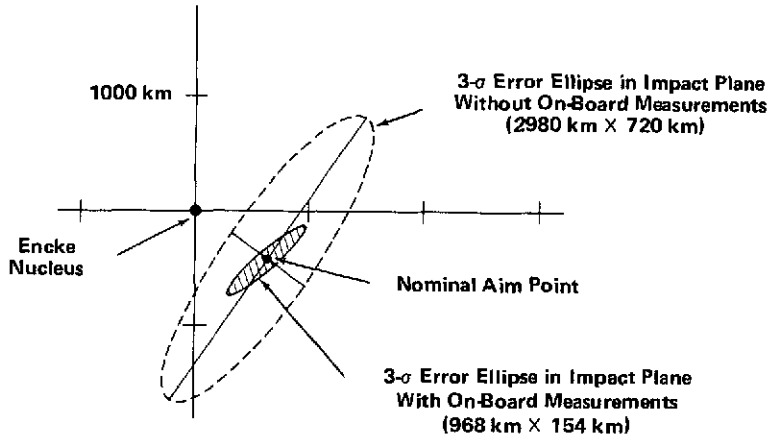

Intercept Date	Dec. 7, 1980	Comet Tracking Assumptions	
Launch Date	Aug. 24, 1980	Spacecraft-based Measurements:	
Spacecraft Position Error at Encounter	20 km (3 σ)	Time Interval	E – 6 to E – 3 Days
		Measurements per Day	2
		Total Measurements	7
		Accuracy	6 arcseconds (1 σ)
		Earth-based Measurements:	See table 2.

Figure 11. Spacecraft targeting errors at encounter.

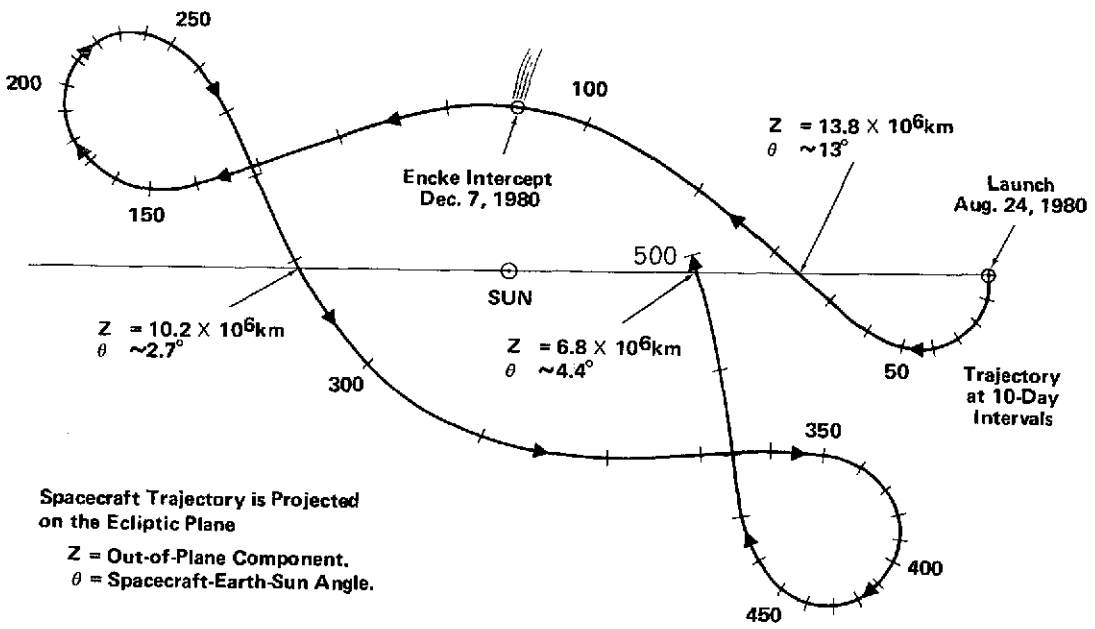

Figure 12. Spacecraft trajectory relative to fixed Sun-Earth line.

There is another important extended-mission objective that merits serious consideration, namely, the attainment of a second encounter with Encke in 1984. This intriguing possibility exists because Encke's orbital period is nearly an exact integral multiple of the spacecraft's orbital period (that is, $T_{ENCKE} \sim 6T_{S/C}$). Therefore, only a slight adjustment of the spacecraft trajectory would be necessary to achieve a second encounter, which would take place at virtually the same point in Encke's orbit as the first encounter. The ΔV-requirements for the retargeting maneuver, covering a representative sample of launch and intercept dates, are given in table 5. Note that the maneuver is executed about 2 to 3 weeks after the first Encke encounter. If the maneuver is delayed until the next small-ΔV opportunity, which occurs just before the spacecraft returns to perihelion, the ΔV costs will increase by approximately 20 meters per second.

In computing the retargeting maneuver, changes in Encke's orbital parameters from 1980 to 1984 (see figure 1) were taken into account, but perturbations of the spacecraft orbit during the same interval were neglected. Computer simulations of the perturbed spacecraft trajectory demonstrated that the error introduced by this approximation was insignificant.

Assuming that one or both spacecraft would still be functioning some 3.6 years after launch, a second near-perihelion intercept of comet Encke would be realized. The two successive intercepts could provide new data concerning the evolution of certain cometary features (for example, relative abundances of coma constituents). Finally, it should be noted that the second Encke encounter would take place when solar activity is near a minimum, whereas the first encounter would have occurred near solar maximum.

SPACECRAFT CONCEPT

The principal guideline used in developing preliminary designs for the coma and tail probes was to utilize conventional spacecraft technology. Flight-proven subsystems were included whenever possible. For example, to satisfy the thermal requirements at 0.34 AU (8.6 solar constants), it was decided to use the thermal-control and power-subsystem designs that have been developed for the Helios spacecraft which will operate at 0.30 AU (11.1 solar constants). The despun-platform design was adopted from the highly successful OSO spacecraft series. This design has achieved pointing accuracies as small as 1.5 arcseconds and has never experienced an inflight failure (reference 21).

Major features and capabilities of the coma and tail probes are given in figure 13. Note the close similarity to the Helios structural design. Except for the despun platform and additional experiments on the coma probe, the two spacecraft are identical. The twin-spacecraft combination is shown in its launch configuration in figure 14.

Both spacecraft are equipped with hydrazine propulsion systems that are used to perform midcourse corrections, attitude control, and spin-rate control. The ΔV-capabilities for the coma and tail probes are 235 and 275 meters per second, respectively. With this capability, at least 170 meters per second can be allocated for the retargeting maneuver that is needed to accomplish the second Encke intercept in 1984.

Table 5
Optimal Retargeting Maneuver for Second Encke Encounter

Intercept Date 1980 (First Encounter)	Launch Date 1980	Period Change ΔT (Days)	Time of Impulse (Days After First Encounter)	ΔV (Meters per second)
Dec. 3	Aug. 30	3.2	11	158
3	Sept. 1	3.4	11	198
3	3	3.7	12	233
4	Aug. 27	2.3	12	103
4	29	2.3	15	142
4	31	2.5	15	190
6	Aug. 24	1.4	22	156
6	26	1.3	21	137
6	28	1.3	19	107
7	Aug. 21	1.3	23	153
7	23	1.1	24	137
7	25	1.0	24	122
8	Aug. 18	1.5	22	164
8	20	1.2	24	146
8	22	0.9	26	131

Because of a possible meteoroid hazard in the vicinity of Encke, some meteoroid shielding will also be required. The most effective meteoroid protection is provided by a double-wall shielding structure. The first wall, which is relatively thin, is used to shatter an incoming particle, creating a diffuse debris cloud. The second wall must withstand only an encounter with this cloud. However, if the velocity of the incoming particle is too low, it will not shatter. This characteristic is illustrated in figure 15 where it can be seen that, except for impact velocities near zero, the maximum protection is obtained at meteoroid speeds of about 7 km/second. This value has been verified by experimental test data (reference 22).

COMPARISON WITH OTHER PROPOSALS

As mentioned in the introduction to this paper, two alternative mission modes have been proposed for the 1980 Encke flyby mission. One plan envisions the use of an as yet undeveloped solar-electric propulsion module to accomplish a slow flyby at 4 km/second. The other mission proposal is constrained to using an Atlas/Centaur launch vehicle, thereby limiting the minimum achievable flyby speed to about 20 km/second. Both of these

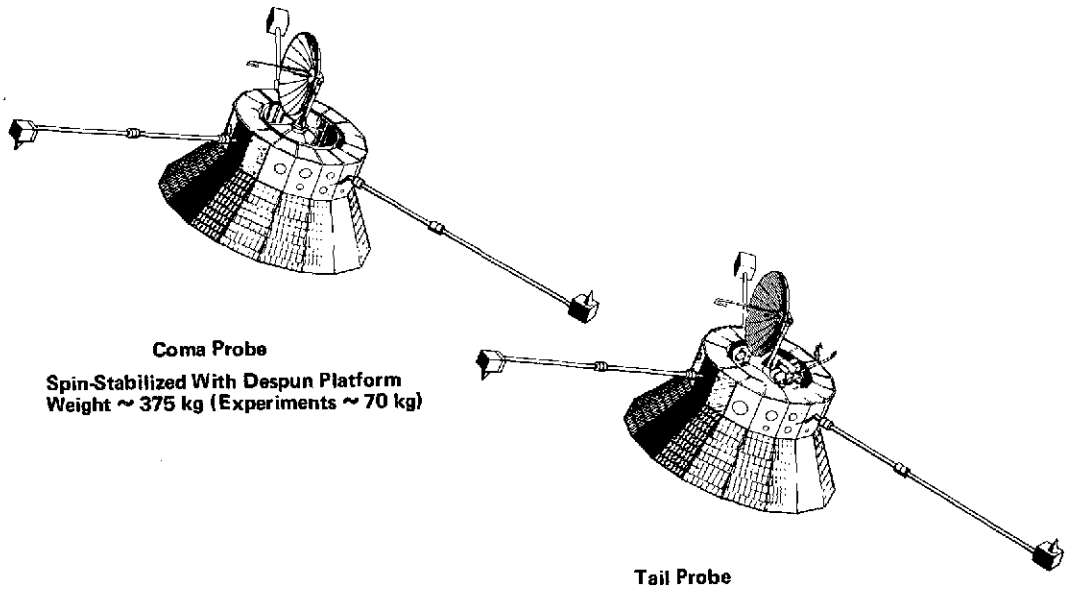

Coma Probe

Spin-Stabilized With Despun Platform
Weight ~ 375 kg (Experiments ~ 70 kg)

Tail Probe

Spin-Stabilized With Despun Antenna
Weight ~ 325 kg (Experiments ~ 35 kg)

Spacecraft Summary

Subsystem Heritage: Helios, Explorer, OSO, ATS.
Spacecraft Magnetically and RFI Clean.
Available Power, ~180 Watts at 1 AU; ~600 Watts at 0.4 AU.
Bit Rate at Encounter, ~4096 bps.
Data Storage Capability, ~10^9 Bits.

Figure 13. Summary of data for the twin spacecraft.

mission modes are discussed below, and their effectiveness is compared with the ballistic slow-flyby mode.

Solar-electric Propulsion Slow-flyby Mission Mode

Because the 1980 Encke slow-flyby mission using solar-electric propulsion (SEP) has been the subject of many papers (see references 23 and 24), only a brief description will be given here. The principal features of this mission mode are outlined in figures 16 and 17. The low relative velocity of only 4 km/second and the small communications distance to earth at intercept are easily the greatest advantages of the SEP mission. However, the intercept takes place some 30 days before Encke reaches its perihelion, where production rates of parent molecules and fluorescent emissions of daughter molecules are far below their perihelion levels. Other major disadvantages of the SEP slow flyby are described below.

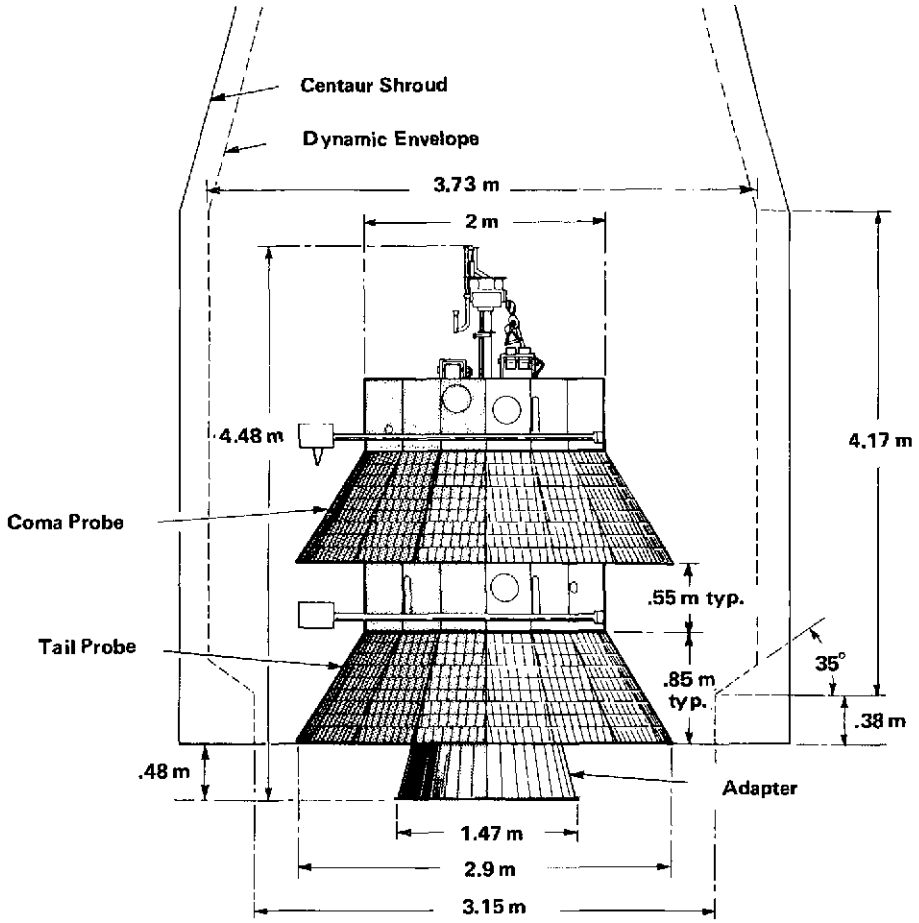

Figure 14. Dual-probe launch configuration.

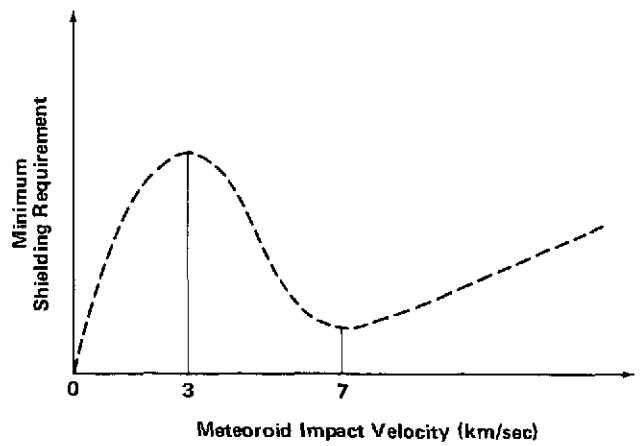

Figure 15. Meteoroid shielding requirement.

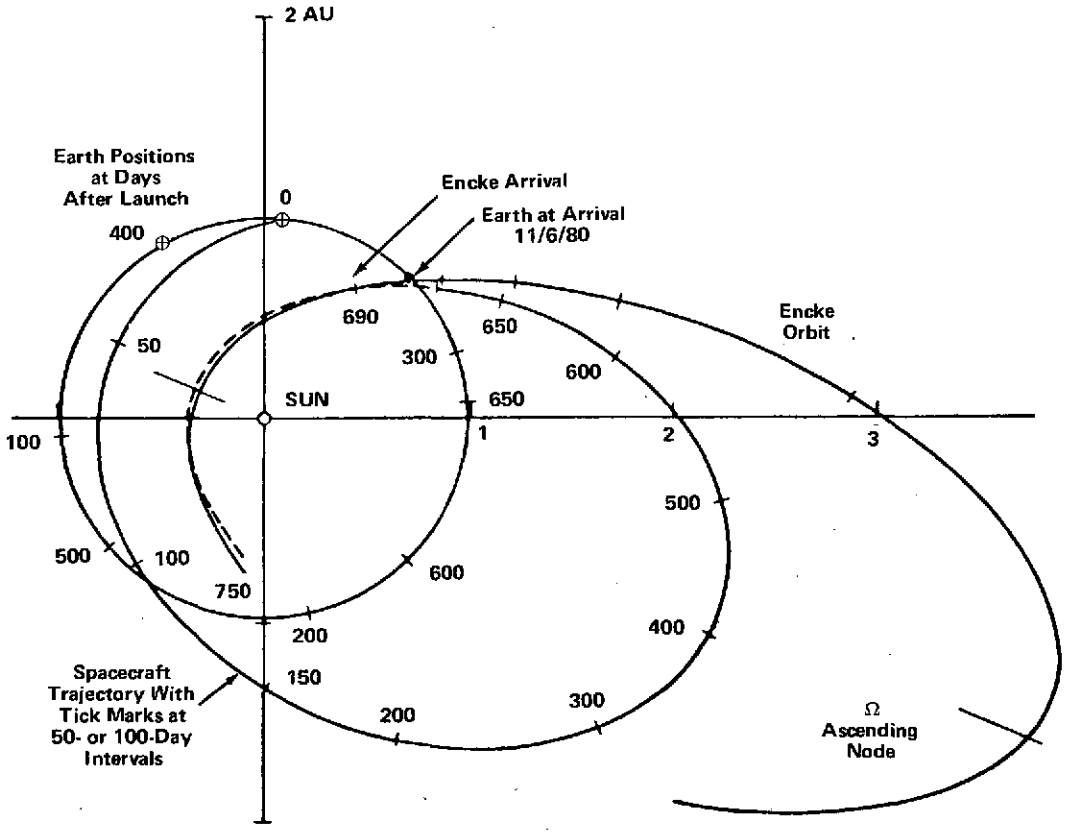

Launch Date	Dec. 17, 1978
Intercept Date	Nov. 6, 1980
Flight Time	690 Days
Launch Vehicle	Titan 3E/Centaur

At Intercept	
Relative Velocity	4 km/sec
Phase Angle	11°
Sun Distance	0.80 AU
Earth Distance	0.33 AU

Transfer Orbit	
Perihelion	0.34 AU
Aphelion	2.43 AU

Spacecraft Summary	
Three-axis Stabilized	
Solar Electric Propulsion	12 kw
Total Weight	1500 kg
Experiment Weight	62 kg

Figure 16. Solar Electric Propulsion (SEP) slow flyby mission.

- Mission success is critically dependent on the performance of a solar-electric propulsion system that has not been flight tested. The 30-cm ion thruster system must operate continuously for almost two years.

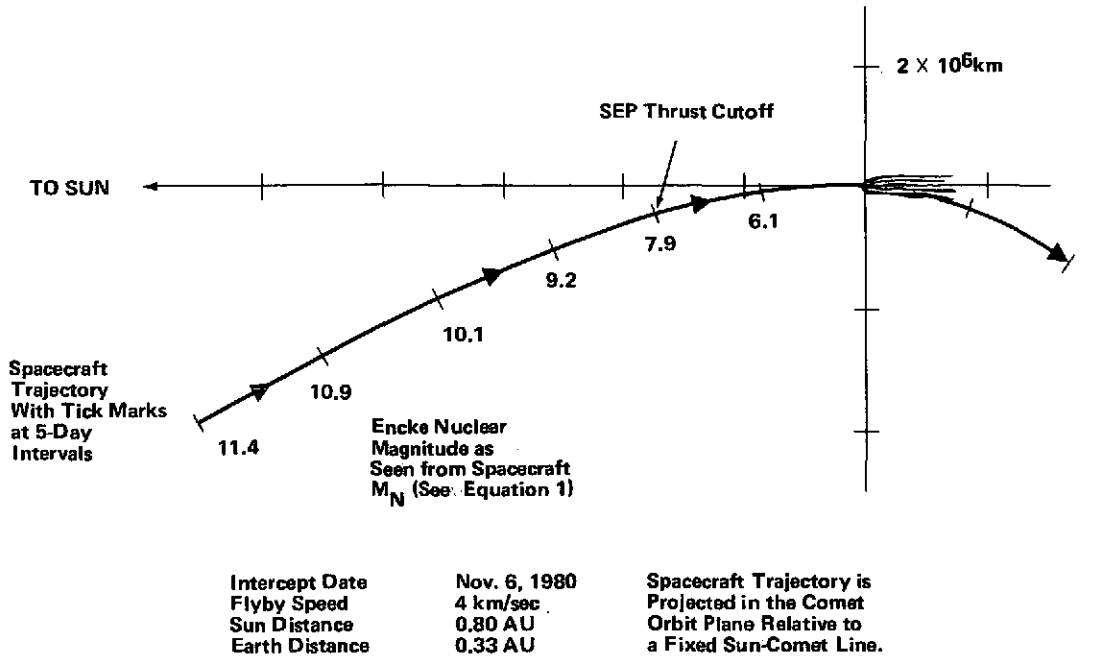

Figure 17. Encounter geometry for SEP slow flyby.

- In reference 25 it was shown that random thrust errors present in the SEP system cause large spacecraft targeting errors at Encke encounter. The detrimental effect of these errors on the science value of the Encke flyby mission is shown in table 6. Notice that the density of parent molecules at the nominal mass distance is about 300 times smaller than the corresponding case for the ballistic slow flyby. Furthermore, the 3500-km nominal miss distance given in table 6 is probably optimistic because it is based on the assumption that onboard optical measurements of Encke's nucleus are available 30 days before encounter. However, figure 17 indicates that Encke's nucleus will not be detected from the spacecraft until roughly 10 days before encounter (assuming a detection threshold of magnitude 8.0).

- Ion-engine contaminant effects will degrade scientific data from particle and field experiments. Some of these contaminant effects will remain even after the ion engine is turned off. As a matter of fact, d.c. electric contamination is expected to be at least an order of magnitude larger after engine shutdown (reference 26).

- As shown in figure 17, the encounter trajectory passes through Encke along its longitudinal axis. This type of trajectory will severely limit spectrophotometric measurements after encounter because the instrument would be looking into the sun. It will also be very difficult to separate space-time variations during the traverse. Some interesting data might be obtained in the tail region, but only an extremely short tail is likely to exist at 0.8 AU.

Table 6
Effect of Targeting Errors on Science Return

		Ballistic Slow Flyby		Ballistic Fast Flyby	SEP Slow Flyby
		With Terminal Guidance	Without Terminal Guidance		
Measurements of Encke's nucleus from spacecraft	Number of Measurements	7	–	–	80
	Time Interval	E-6 Days to E-3 Days	–	–	E-30 Days to E-10 Days
Miss Distance (3–σ) (km)	Nominal	480	760	880	3500
	Maximum	680	1700	1600	6600
Number density of parent molecules (H_2O)* at closest approach (number per cm^3)	At Nominal Miss Distance	1.2×10^7	4.8×10^6	1.3×10^6	4.1×10^4
	At Maximum Miss Distance	6.0×10^6	9.6×10^5	3.8×10^5	1.1×10^4
Nominal S/C residence time in region where densities of parent molecules (H_2O) are greater than 10^5 per cm^3 (minutes)		18.6	18.5	4.8	0

*Densities of C_2 and CN are several hundred times smaller. Detection threshold for neutral mass spectrometer is approximately 10^3 molecules per cm^3.

- The SEP spacecraft is three-axis stabilized and is not designed to function in a high-temperature thermal environment. Therefore, the possibility that the SEP spacecraft will survive its perihelion passage at 0.34 AU seems remote. A probable curtailment of the SEP mission about one month after the Encke encounter does not compare favorably with the attractive extended-mission scientific opportunities that are available with the ballistic slow flyby.

In summary, it appears that the science return from the 1980 Encke flyby mission would be reduced significantly if the SEP mode is employed.

Ballistic Fast-flyby Mission Mode

Studies of a ballistic fast flyby of comet Encke in 1980 have been carried out because of a desire to find out if acceptable science return could be achieved with a Pioneer-class

spacecraft and an Atlas/Centaur launch vehicle. The main characteristics of this mission mode are given in figures 18 and 19. Further details can be found in reference 27. Because the first acquisition of Encke's nucleus from the spacecraft will not occur until three days before encounter (again assuming a detection threshold of magnitude 8.0), insufficient time will be available for terminal-guidance operations.

With the exception of the relatively small communications distance at intercept, it is difficult to find merit in this proposal. Some of the main objections to the ballistic fast-flyby mode are listed below.

- The encounter velocity of 20 km/second is simply too fast. In table 6 it can be seen that the spacecraft residence time in a region where parent-molecule densities are greater than 10^5 per cm^3 would be less than 5 minutes. Furthermore, the probability of neutral-molecule impact fragmentation is quite high at a relative velocity of 20 km/second. The high encounter velocity also increases the chances of spacecraft damage from particulate matter in the vicinity of Encke (see figure 15).

- The Atlas/Centaur/TE 364-4 launch vehicle does not possess sufficient payload capability for the 1980 Encke flyby mission. For an intercept on November 18, 1980, the total spacecraft weight cannot exceed 340 kg. If, as recommended in reference 27, the Pioneer spacecraft is equipped with a despun platform and a small coma probe is included, the spacecraft weight will total almost 420 kg.

- The rationale for choosing the encounter trajectory shown in figure 19 is that extensive measurements in Encke's tail region would be possible. However, Encke's visible tail is quite narrow, and the encounter phase angle of 5° coupled with an uncertainty in the aberration angle of Encke's tail of about 11° suggests that the anticipated measurements in the distant tail region may be more of a hope than a reality.

- Assuming that the imaging system cannot be pointed towards an object that is located within 50° of the sun's limb, the time available for close-range imaging of Encke's nucleus will shrink further. For the nominal miss distance of 880 km, the maximum imaging time at distances smaller than 10^4 km from the nucleus is only 8.9 minutes. The time available for close-range imaging in the ballistic slow-flyby mode is about 41.6 minutes, which is almost 5 times longer.

CONCLUDING REMARKS

From the foregoing discussion, it is clear that the full science value of the 1980 Encke flyby mission can only be realized by adopting the ballistic slow-flyby mode. This mission mode offers a unique opportunity for obtaining high-quality in situ measurements of comet Encke near its perihelion where it is most active. Some of the desirable features of the ballistic slow flyby are the following.

- Flyby speeds of only 7 to 9 km/second coupled with short flight times (~100 days).

Launch Date	Aug. 18, 1980
Intercept Date	Nov. 18, 1980
Flight Time	92 Days
Launch Vehicle	Atlas/Centaur/TE-364-4

At Intercept

Relative Velocity	20.1 km/sec
Phase Angle	5.1°
Sun Distance	0.57 AU
Earth Distance	0.52 AU

Transfer Orbit

Perihelion	0.49 AU
Aphelion	1.0 AU

Spacecraft Summary

Spin-Stabilized	
Total Weight	340 kg
Experiment Weight	55 kg

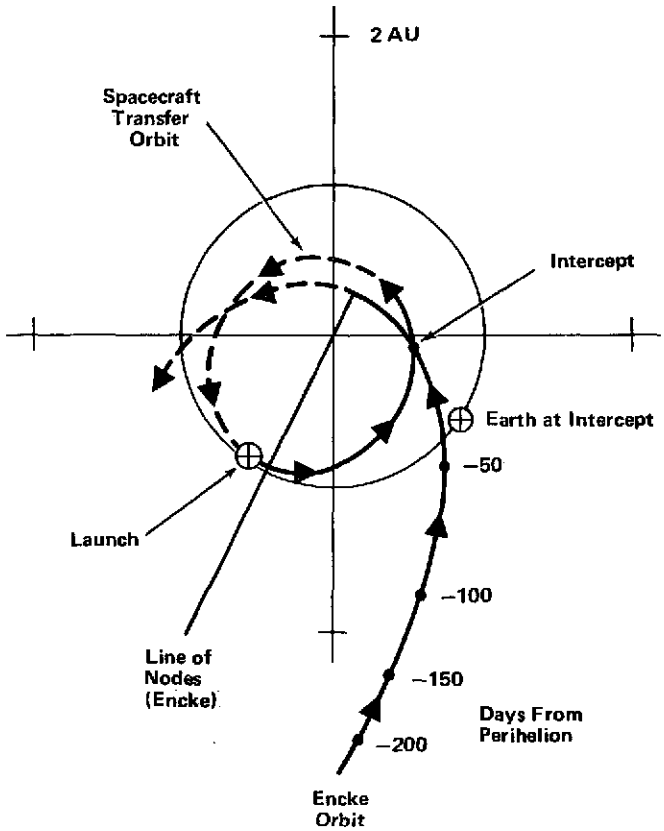

Figure 18. Ballistic fast-flyby mission mode.

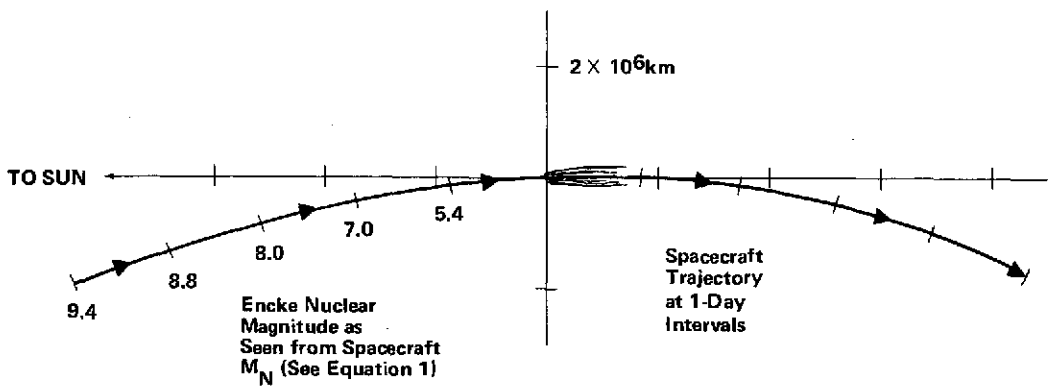

Intercept Date	Nov. 18, 1980	Spacecraft Trajectory is
Flyby Speed	20.1 km/sec	Projected in the Comet
Sun Distance	0.57 AU	Orbit Plane Relative to
Earth Distance	0.52 AU	a Fixed Sun-Comet Line.

Figure 19. Encounter geometry for ballistic fast flyby.

- Small targeting errors at encounter assuring extended in situ measurements in Encke's inner coma where molecular densities are high.
- Excellent encounter geometry permitting spectrophotometric measurements of the coma/tail region before and after encounter. The fortuitous geometrical situation also leads to multiple crossings of the bow shock and contact surface.
- Unusually good opportunities for additional science return after the Encke intercept including a second encounter with Encke in 1984.

The attractiveness of the ballistic slow-flyby mode is enhanced further by incorporating the twin-probe intercept strategy. Some of the added benefits made possible with this plan are that:

- Simultaneous measurements will be taken in Encke's coma and tail regions.
- Planned experiment weight is 105 kg (70 kg for the coma probe and 35 kg for the tail probe).
- Probability of mission success is increased by the redundancy that is inherent in the twin-probe concept.

ACKNOWLEDGMENT

We would like to thank our GSFC colleagues L. Burlaga, B. Donn, M. Mumma, and N. Ness for many useful discussions concerning the scientific aspects of the Encke flyby mission.

Goddard Space Flight Center
National Aeronautics and Space Administration
Greenbelt, Maryland February 1974
684-39-10-01-51

REFERENCES

1. System Definition for Cometary Explorer, NASA TM X-70561, November 1973.

2. Farquhar, R. W., and N. F. Ness, "Two Early Missions to the Comets," *Astronaut. and Aeronaut.*, **10**, No. 10, October 1972.

3. Kuiper, G. P., and E. Roemer, eds., *Proc. of the Tucson Comet Conference*, Univ. of Arizona, Tucson, Arizona, 1972.

4. Roberts, D. L., ed., *Proc. of the Cometary Science Working Group*, Yerkes Observatory, Williams Bay, Wisconsin, 1971.

5. *The 1973 Report and Recommendations of the NASA Science Advisory Committee on Comets and Asteroids*, NASA TM X-71917, 1973.

6. Bertotti, B., and G. Colombo, "Precision Measurement of the Sun's Gravitational Field by Means of the Twin Probe Method," *Astrophys. and Space Sci.*, **17**, 1972, pp. 223-237.

7. Kresák, L., "On the Secular Variations in the Absolute Brightness of Periodic Comets," *Bulletin of the Astronomical Institutes of Czechoslovakia*, **16**, No. 6, 1965.

8. Sekanina, Z., *Secular Decrease in the Absolute Brightness of the Comet Encke*, NASA TT F-599, June 1970, pp. 43-62.

9. IAU Circular No. 1867, 1964.

10. Marsden, B. G., "Periodic Comet Encke," IAU Circular No. 2547, 1973.

11. Sekanina, Z., "A Model for the Nucleus of Encke's Comet," *Proceedings of IAU Symposium No. 45*, 1972, pp. 301-307.

12. Whipple, F. L., "Brightness Changes in Periodic Comets," *Astron. J.*, **69**, No. 2, 1964, p. 152.

13. Sekanina, Z., "Dynamical and Evolutionary Aspects of Gradual Deactivation and Disintegration of Short-Period Comets," *Astron. J.*, **74**, No. 10, 1969.

14. Whipple, F. L., and S. E. Hamid, "A Search for Encke's Comet in Ancient Chinese Records: A Progress Report," *Proc. of IAU Symposium No. 45*, 1972, pp. 152-154.

15. Marsden, B. G., and Z. Sekanina, "Comets and Nongravitational Forces, VI. Periodic Comet Encke 1786-1971," *Astron. J.*, 1974.

16. Yeomans, D. K., "The Nongravitational Motion of Comet Kopff," *Publications of the Astronomical Society of the Pacific*, February 1974.

17. Bertaux, J. L., J. E. Blamont, and M. Festou, "Interpretation of Hydrogen Lyman-Alpha Observations of Comets Bennett and Encke," *Astron. and Astrophys.*, **25**, 1973, pp. 415-430.

18. Delsemme, A. H., "Comets: Production Mechanisms of Hydroxyl and Hydrogen Halos," *Science*, **172**, 1971, pp. 1126-1127.

19. Acton, C. H., "Processing Onboard Optical Data for Planetary Approach Navigation," *J. Spacecraft & Rockets*, 9, No. 10, October 1972.

20. Thorpe, T. E., "Mariner-9 Star Photography," *Appl. Opt.*, 12, No. 2, February 1973.

21. Follett, W. H., and T. M. Spencer, "Description and In-Orbit Performance of the Orbiting Solar Observatory Control System," *AIAA Paper No. 72-852*, August 1972.

22. Howard, J. R., "Development of the Mariner Mars 1971 Meteoroid Shield," *J. Spacecraft & Rockets*, 7, No. 1, January 1970.

23. Bender, D. F., K. L. Atkins, and C. G. Sauer, "Mission Design for a 1980 Encke Slow Flyby Using Solar Electric Propulsion," Presented at AAS/AIAA Astrodynamics Conference, July 1973.

24. Sauer, C. G., "Trajectory Analysis and Performance for SEP Comet Encke Missions," *AIAA Paper No. 73-1059*, October 1973.

25. Jacobson, R. A., J. P. McDanell, and G. C. Rinker, "Terminal Navigation Analysis for the 1980 Comet Encke Slow Flyby Mission," *AIAA Paper No. 73-1063*, October 1973.

26. Sellen, J. M., "Causes and Control of Solar Electric Propulsion Interactive Effects," *AIAA Paper No. 73-1127*, October 1973.

27. Bursnall, W. J., E. G. Howard, W. R. McMinimy, R. G. Shaffer, and J. M. Van Pelt, *Study of 1980 Comet Encke-Asteroid Missions Using a Spin-stabilized Spacecraft*, NASA CR-114671, October 1973.

NASA-Langley, 1974